Microchimica Acta (2020) 187: 388
https://doi.org/10.1007/s00604-020-04362-z

ORIGINAL PAPER

Magnetic organic porous polymer as a solid-phase extraction adsorbent for enrichment and quantitation of gastric cancer biomarkers (P-cresol and 4-hydroxybenzoic acid) in urine samples by UPLC

Shanshan Li[1] · Yintang Zhang[2] · Shuai Mu[1] · Minrui Ma[1] · Xiaoyan Liu[1] · Haixia Zhang[1]

Received: 14 January 2020 / Accepted: 31 May 2020 / Published online: 15 June 2020

Abstract

A novel magnetic organic porous polymer (denoted as Fe_3O_4@PC-POP) was developed for magnetic solid-phase extraction (MSPE) of two gastric cancer biomarkers (P-cresol and 4-hydroxybenzoic acid) from urine samples prior to high-performance liquid chromatographic analysis. The adsorbent was characterized by scanning electron microscope, transmission electron microscope, FTIR, powder X-ray diffraction, and other techniques. The result of dynamic light scattering shows that the particle size of the adsorbent is mainly distributed around 400 nm. Based on the design concept of the Fe_3O_4@PC-POP, the proposed material can effectively capture the target analytes through electrostatic and hydrophobic interaction mechanism. Furthermore, the enrichment conditions were optimized by the response surface method, and the method was utilized for the determination of P-cresol and 4-hydroxybenzoic acid in real urine samples from health and gastric cancer patients with high enrichment factors (34.8 times for P-cresol and 38.7 times for 4-hydroxybenzoic acid), low limit of detection (0.9–5.0 μg L^{-1}), wide linear ranges (3.0–1000 μg L^{-1}), satisfactory relative standard deviation (2.5%–8.5%), and apparent recoveries (85.3–112% for healthy people's and 86.0–112% for gastric cancer patients' urine samples). This study provides a guided principle for design of the versatile polymer with specific capturing of the target compounds from complex biological samples.

Keywords Gastric cancer · Biomarkers · Fe_3O_4@PC-POP · P-cresol · 4-Hydroxybenzoic acid

Introduction

Gastric cancer is the common malignant tumors of the digestive tract, with high morbidity and mortality. One of the most important reasons for such high mortality is that most of gastric cancer patients have no specific symptoms in early-stage gastric cancer [1, 2]. Therefore, good biomarkers are essential to the early diagnosis of gastric cancer [3–6]. Recently, significant progresses have been achieved in the screening of potential metabolite biomarkers for gastric cancer from urine samples [7–9]. In these studies, some small molecule metabolites including amino acids, altered lipid metabolism, as well as organic metabolites were listed as potential urinary biomarker for gastric cancer. Among them, proline and other two organic metabolites (P-cresol and 4-hydroxybenzoic acid) should be paid more attention owing to their high correlation with survival rate [9]. Therefore, establishment of a simple method for analysis of them can aid in the early diagnosis, prognosis, and promoting the understanding of the pathogenic mechanisms. However, since the levels of them are prone to relatively low in urine samples, it is necessary to develop a sample pretreatment technique to reduce the complexity of sample and further improve the determination sensitivity prior to analysis.

Electronic supplementary material The online version of this article (https://doi.org/10.1007/s00604-020-04362-z) contains supplementary material, which is available to authorized users.

✉ Xiaoyan Liu
liuxiaoy@lzu.edu.cn

[1] State Key Laboratory of Applied Organic Chemistry, Key Laboratory of Nonferrous Metals Chemistry and Resources Utilization of Gansu Province and College of Chemistry and Chemical Engineering, Lanzhou University, Lanzhou 730000, China

[2] Henan Key Laboratory of Biomolecular Recognition and Sensing, College of Chemistry and Chemical Engineering, Shangqiu Normal University, Shangqiu 476000, China

To date, several approaches aimed at metabolite biomarkers have been developed by different techniques coupled to GC-MS [9, 10], UHPLC-MS [11, 12], and LC-MS [13, 14]. In addition, there are some existing analytical methods to assay 4-hydroxybenzoic acid and phenolic compounds, respectively. For example, Kashani used the sensor consists of a carbon paste electrode modified with nickel titanate nanoceramics ($NiTiO_3$/CPE) to determine the preservative products para-hydroxybenzoic acid (PHB) in wastewater samples [15]. Carolina synthesized a hybrid material made of β-cyclodextrin anchored to a polymeric network as a sorbent for solid-phase extraction of phenolic compounds [16]. Among these studies, except the previous report on screening gastric cancer biomarkers [9], there is only one case report regarding the simultaneous determination of P-cresol and 4-hydroxybenzoic acid by means of a magnetic polymer based on β-cyclodextrin as a solid-phase extraction material [17]. These works further offer the possibilities of P-cresol and 4-hydroxybenzoic acid as metabolite biomarkers for conventional diagnosis of gastric cancer. However, considering the complexity of the actual sample matrix, the progress in the practical application is still insufficient, and further exploration of some more effective and lower cost enrichment materials than traditional adsorbents for treatment of these target compounds is imperative.

Porous organic polymer networks (POPs) is a type of pure organic structural building units based on light elements (C, B, H, O, N) assembled by strong covalent bonds, with a highly porous cross-linked nanostructure polymer [18]. Recently, the intriguing features including abundant porosity, adjustable chemical structure, and excellent physical and chemical stability of POPs also drive its potential application in separation and analysis [19–21]. Further, due to the abundant functional monomer of POPs, a large number of POPs have been synthesized with different principles to separate and enrich different substances [22, 23]. Therefore, in order to improve the performance of adsorbent for metabolites biomarkers, it is necessary to synthesize building monomers with different structures depending on the nature of the analytes.

Magnetic solid-phase extraction (MSPE), a solid-phase extraction (SPE) mode based on magnetic or magnetically modified adsorbents, has been developed as a promising preenrichment and separation technique [22, 24]. In the MSPE process, the analytes can be quickly adsorbed onto the magnetic adsorbent from the sample solution and then collected by an external magnetic field, which greatly simplifies the sample pretreatment process and improves the extraction efficiency [25]. Therefore, the development of a new type of high-efficiency adsorbent with magnetic separation function is of great importance.

Herein, we designed a new Fe_3O_4@PC-POP ("PC" stands for two reactants piperazine and cyanuric chloride) via introducing triazine ring and piperazine units by a facile one-pot strategy. Based on the design concept, the Fe_3O_4@PC-POP possesses positively charged nitrogen-rich structure and hydrophobic triazine ring. In addition, it has a higher specific surface area than other amorphous polymers [26–28]. Thus, the proposed material can be used as a magnetic adsorbent to extract negatively charged and hydrophobic small molecular metabolic markers (P-cresol and 4-hydroxybenzoic acid). The extraction performance was systematically studied, and ultra-high pressure liquid chromatography (UPLC) coupled with UV detector was utilized for accurate determination of P-cresol and 4-hydroxybenzoic acid. The single factor experimental group and the response surface experimental group were designed to evaluate the influence of experimental parameters. Furthermore, the analytical method is applied to assay the two small molecular metabolic markers in actual urine samples from the healthy people and gastric cancer patients. Finally, the metabolic biomarker level differences between healthy people's urine samples and gastric cancer patients' urine samples were also evaluated.

Experiment

Materials

Cyanuric chloride, anhydrous piperazine, P-cresol and 4-hydroxybenzoic acid (Energy Chemical Technology Co., Ltd., Shanghai, China, www.energy-chemical.com); ferric oxide nanoparticles and potassium bromide (Aladdin Reagent Co., Ltd., Shanghai, China, www.aladdin-e.com); 1,4-Dioxane, absolute ethanol, and anhydrous methanol (Chron Chemicals, Sichuan, China, www.cdkelongchem.com); acetonitrile (ACN), acetic acid, phosphoric acid boric acid, sodium chloride, and anhydrous potassium carbonate (Damao Chemical Reagent Factory, Tianjin, China, www.dmreagent.com); and commercial strong anion exchange material (SAX) and Cleanert C18 (Agela Technologies Co., Tianjin, China, www.agela.com.cn).

Instruments and apparatus

The infrared spectrum of the Fe_3O_4@PC-POP material was measured by a Fourier Transform Infrared Spectrometer (Bruker Optics Vertex 70, Germany). The morphology of the materials was characterized by scanning electron microscopy (SEM) (Japan Hitachi, S-4800) and field emission transmission electron microscopy (TEM) (US FEI, Tecnai G2 F30). The magnetic strength of the material was measured by a vibrating sample magnetometer (VSM) (LDJ Electronics, LD J9600-1). The specific surface area and pore size distribution of the materials were characterized by a fully automatic specific surface area and void fraction meter (Micromeritics TriStar 3020, USA). The specific surface area

was calculated by the Brunauer-Emmett-Teller (BET) multipoint method, and the pore size distribution was calculated by the Barrett-Joyner-Halenda (BJH) method. The zeta potentials of material at different pH value were measured using a Zetasizer Nano ZS (zeta potential tester) (NanoBrook 90plus PALS, USA). The chromatographic analysis was performed by Thermo Fisher's Dionex UltiMate 3000 UHPLC equipped with LPG-3400RS Quaternary Analysis Pump, WPS-3000RS Autosampler, TCC-3000RS Column Thermostat, DAD-3000RS Detector, and Thermo Scientific's Chromeleon Chromatography System controlling software. The column was a reverse-phase C18 column (3.5 μm, 4.6 × 100 mm, ZORBAX Eclipse Plus). The chromatographic conditions were as follows: isocratic elution (A = acetonitrile, B = formic acid buffer, 0.1% formic acid; A = 40%, B = 60%); flow rate of 0.8 mL min^{-1}; the detection wavelength for each compound was 4-hydroxybenzoic acid at 250 nm and P-cresol at 280 nm. The injection volume was 20 μL, and all solutions were filtered through 0.22-μm membrane filters.

Preparation of samples

The standard mixture solution of 1.0 mg mL^{-1} for each of P-cresol and 4-hydroxybenzoic acid was prepared in methanol and stored at 4 °C. Then the standard solution was diluted with ultrapure water or Britton-Robinson buffer (B-R) with a certain pH to the desired concentrations and obtained the sample solution for further experiments.

Synthesis of the Fe_3O_4@PC-POP

As shown in Fig.1, Fe_3O_4@PC-POP was synthesized, referring to the method in reference [29], with minor modification. And specific synthesis process is described in the electronic supplementary material (ESM).

MSPE procedure

A certain amount of Fe_3O_4@PC-POP was dispersed into 40.0 mL of diluted artificial urine with each analyte concentration of 2.0 μg mL^{-1} (diluted 8 times by BR buffer at pH 6.0). The mixture solution was shaken at 250 times min^{-1} in a shaker for 1.0 h at 25 °C. Then the supernatant was removed by magnetic separation, and 1.0 mL ethanol (containing 1.0% (v/v) acetic acid, which was added twice) was put into the isolated MSPE sorbents. Subsequently, the twice obtained eluent was mixed and dried under N_2 at 45 °C. The residue was dissolved in 100 μL mobile phase (acetonitrile: H_2O = 40:60 (v/v)) and filtered through 0.22 μm membrane filters. Finally, 20 μL of the filtrate solution was injected into the chromatographic system.

Optimization of extraction conditions

First, the desorption conditions including desorption composition (acetone, methanol, ethanol), acetic acid proportion (0.5%, 1%, 5%, 10%, respectively), desorption volume (interval from 1.0 to 4.0 mL), and desorption time (interval from 3.0 to 10 min) were optimized, respectively.

Second, the extraction conditions were optimized through the response surface optimization method. Briefly, four main factors such as the extraction pH, the salt concentration, the extraction time, and the amount of adsorbent were selected, and the coarse range of each factor was defined. Furthermore, the four-factor and three-level test forms were obtained through the Box-Behnken center combination experiment design. The lowest, intermediate, and highest values of the three

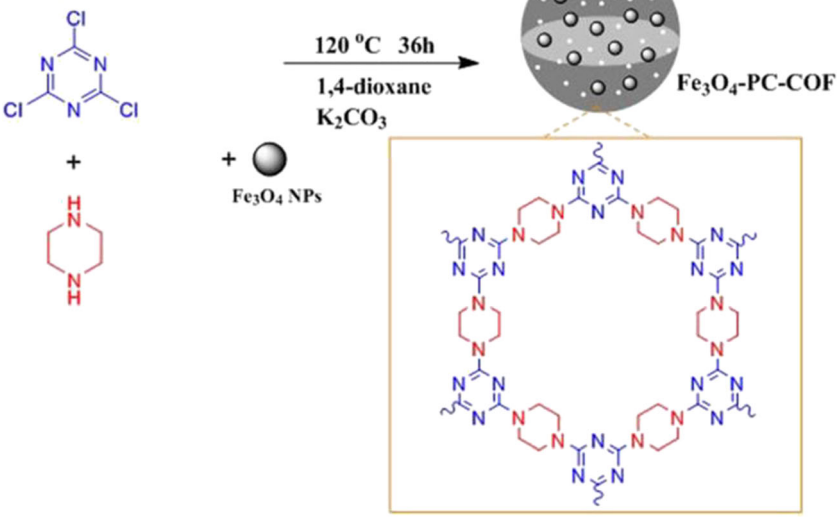

Fig. 1 Schematic of preparation of Fe_3O_4@PC-POP

levels were respectively encoded as − 1, 0, and 1 (see Table 1). Finally, the experimental results were simulated by Design-Expert.V8.0.6.1 software.

Adsorption studies

Adsorption kinetics was tested in 40 mL of 4-hydroxybenzoic acid and p-cresol (200 μg mL^{-1}, pH = 6.0) solution with 50 mg Fe_3O_4@PC-POP. After shaking with different times ranging from 10 to 150 min, the supernatant was separated and determined. Furthermore, adsorption isotherm was tested in 10 mL of analytes solution in different initial concentrations (20–600 μg mL^{-1}) with 15 mg Fe_3O_4@PC-POP at adsorption equilibration time (30 min) to evaluate the adsorption capacity of Fe_3O_4@PC-POP.

Sample analysis

Real urine samples (morning urine) of thirty-three gastric cancer patients and fifteen healthy volunteers were obtained from the clinical laboratory in Second Hospital of Lanzhou University. This study was approved by the ethics committee of the Second Hospital of Lanzhou University. Gastric cancer patients and healthy volunteers participated in this study through verbal consent and anonymity; the experiment guarantees that no privacy of the participants will be disclosed. These samples were stored at −20 °C and assayed within a week. Before use, the samples were thawed at room temperature and centrifuged for 5 min at 10,000 rpm. A 5.0 mL of the supernatant was collected and diluted 8 times with BR buffer (pH = 6.0). Finally, the SPE procedure was carried out as described in the section "MSPE procedure".

In addition, the urine samples of some gastric cancer patients and healthy volunteers were spiked at low, medium, and high concentration of P-cresol and 4-hydroxybenzoic acid (50, 200, 800 μg L^{-1} for P-cresol and 15, 200, and 800 μg L^{-1} for 4-hydroxybenzoic acid), and the apparent recoveries of these analytes were measured by SPE procedure.

Table 1 Box-Behnken center combined experimental design factors and levels

Symbol	Experimental factor	Factor level and coding		
		− 1	0	1
A	pH	3.0	6.0	9.0
B	NaCl (%)	0.0	0.5	1.0
C	Time (min)	20	40	60
D	Adsorbent (mg)	30	55	80

Results and discussion

Characterization of Fe_3O_4@PC-POP

The FT-IR spectra of cyanuric chloride, piperazine, and Fe_3O_4@PC-POP are shown in Fig. S1. The spectrum of Fe_3O_4@PC-POP does not show the N–H stretching vibration of piperazine at 3214 cm^{-1} and the C–Cl stretching mode of cyanuric chloride at 850 cm^{-1}, respectively [30]. In addition, the characteristic band at 806 cm^{-1} indicates the existence of a triazine unit in Fe_3O_4@PC-POP [31]. Furthermore, the existence of the aromatic C=N stretching vibration (1550 cm^{-1} for triazinyl C=N), the aromatic C–N stretching vibrations (1232 cm^{-1}, 1298 cm^{-1}, and 1365 cm^{-1}), and the C–H stretching vibrations (2850 cm^{-1} and 2924 cm^{-1}) of piperazine indicates that both piperazine and triazine units are included in Fe_3O_4@PC-POP [32–36]. These data confirm the successful synthesis of the material.

The XRD pattern (Fig. S2) shows that Fe_3O_4@PC-POP is amorphous polymer with three characteristic diffraction peaks for Fe_3O_4 (2θ = 30.2°, 35.6°, and 43.2°).

Figure 2 shows the SEM and TEM images of PC-POP and Fe_3O_4@PC-POP. As shown in Fig. 2a and b, the material has relatively uniform, spherical porous structural properties. The size of the nanoparticles is approximately 400 nm. As shown in Fig. 2c and d, the morphology of PC-POP presents a sunflower-like core-shell structure. After modification, some Fe_3O_4 nanoparticles were dispersed on PC-POP to form Fe_3O_4@PC-POP, which indicates the successful synthesis of the magnetic material Fe_3O_4@PC-POP. In addition, according to the EDAX mapping of Fe_3O_4@PC-POP (Fig. S4), Fe and O atoms from the incorporated Fe_3O_4 nanoparticles are relatively uniformly distributed on the C and N atoms of the triazine ring and the piperazine units.

Table S1 lists the specific surface area, adsorption and desorption cumulative pore volume, and average pore size parameters of PC-POP and Fe_3O_4@PC-POP. The result shows that PC-POP has a relatively large surface area. However, the specific surface area decreases sharply after the magnetic modification. It heralds that PC-POP is doped with a low specific surface area Fe_3O_4 and the complex Fe_3O_4@PC-POP is formed. According to the nitrogen adsorption-desorption isotherm of PC-POP and Fe_3O_4@PC-POP (Fig. S4), the type IV isotherm has a hysteresis loop from P/P_0 = 0.1 to 1.0, indicating that the material possesses a highly uniform mesoporous structure with a pore size of about 7 nm, which increase the adsorption sites of the material.

According to the elemental analysis of the polymer (Table S2), the content (%) of N, C, and H is 36.3, 45.9, and 5.08, respectively. A rich nitrogen atom in the framework of PC-POP provides a possible positively charged surface, and it enables enrichment of the protonizable 4-hydroxybenzoic acid. However, with regard to P-cresol, it should depend on the

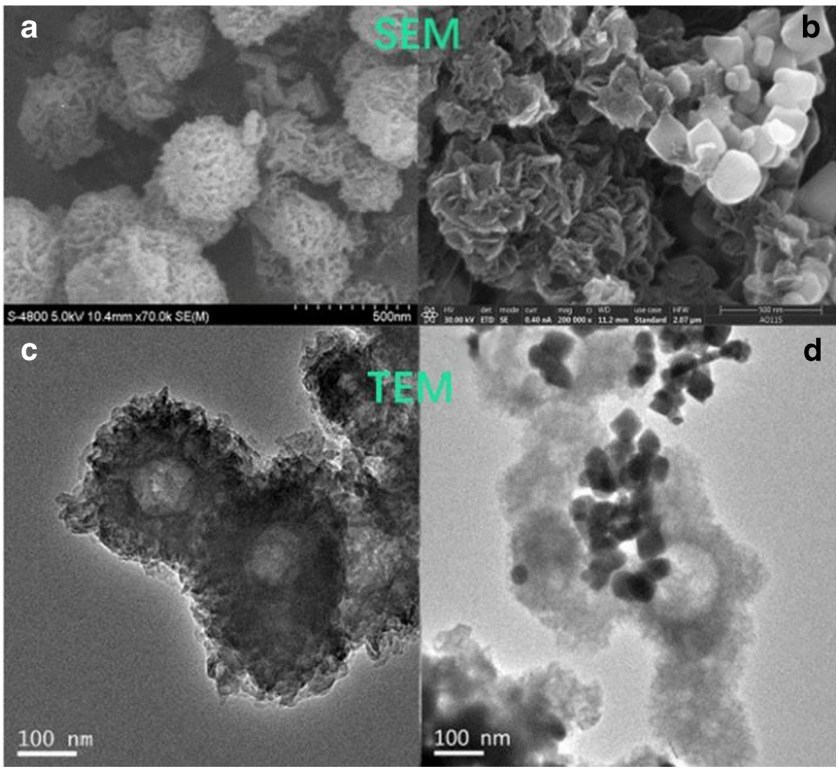

Fig. 2 SEM and TEM images of PC-POP (**a, c**) and Fe_3O_4@PC-POP (**b, d**)

hydrophobic triazine structure of PC-POP to perform the adsorption process. In this case, an appropriate pH environment should be provided for extraction of 4-hydroxybenzoic acid and P-cresol.

To verify charge properties of the material under the different conditions, the material Fe_3O_4@PC-POP was dispersed in deionized water and B-R buffer solutions with different pH values. Figure S5 shows that the zeta potential value of Fe_3O_4@PC-POP tends to decrease progressively with an increasing pH of the buffer solution and Fe_3O_4@PC-POP in B-R buffer solution at pH =4.0 shows zero zeta potential.

From the above perspective, the hydrophobicity of the material should also be presented in the adsorption process. Figure S6 shows that the static water contact angles of Fe_3O_4 and Fe_3O_4@PC-POP are about 100° and 133°, respectively. According to SEM and TEM of Fe_3O_4@PC-POP, the enhancement of hydrophobicity of material is mainly derived from the combination of PC-POP and Fe_3O_4.

The vibrating sample magnetization (VSM) curves of Fe_3O_4 nanoparticles and magnetic Fe_3O_4@PC-POP are shown in Fig. S7. As shown in Fig. S8, the saturation magnetizations of Fe_3O_4 and Fe_3O_4@PC-POP are 73.31 and 49.46 emu g^{-1}, respectively, indicating that the magnetic properties of PC-POP are decreased after magnetic modification. However, the material still has strong magnetic properties and can be quickly separated from the solution by applying an external magnetic field after modification (see the inset of Fig. S7).

Optimization of operation conditions

Optimization of desorption conditions

In order to achieve the high enrichment efficiency, the type of desorption solvent, the volume of the desorption solution, and the desorption time are optimized, respectively. As shown in Fig. S8, the desorption time of 5 min and the desorption solvent of 2.0 mL were selected. Considering that an interaction between the organic solvent and the acid concentration may occur in the desorption process, acetonitrile, methanol, and ethanol solutions containing different concentrations of acetic acid (0.5%, 1%, 5%, and 10%) were used as desorption solvent to be investigated, respectively. As shown in Fig. S9, the trend of the desorption performance of desorption solvent with different acetic acid concentrations is similar, indicating that there is no interaction. However, compared with acetonitrile and methanol, ethanol containing 5% acetic acid as desorption solvent has relatively higher desorption efficiencies for the target compounds. Therefore, ethanol containing 5% acetic acid is selected as the final desorption solvent.

Optimization of extraction conditions by response surface methodology

Several parameters such as pH, amount of adsorbent, extraction time, and ionic strength were optimized. The experimental results were processed by the response surface data

processing software and the regression model variance analysis (Table S3). Considering the overall responses of both 4-hydroxybenzoic acid and P-cresol, the average peak area of 4-hydroxybenzoic acid and P-cresol was used to evaluate the extraction conditions. Figure S10 shows that the optimal extraction conditions for two target compounds are pH = 5.5, salt concentration of 0.0%, extraction time of 60 min, and the sorbents amount of 49 mg. Under these conditions, the predicted average peak area of the two analytes is 40.7 mAu*Sec. The actual average peak area of the two analytes is 40.2 mAu*Sec. Compared with the theoretical prediction value, the relative error is about 1.2%, which indicates that the regression equation obtained by response surface optimization is accurate and reliable.

Performance studies of Fe_3O_4@PC-POP

Figure 3 shows the adsorption kinetic and adsorption isotherm of Fe_3O_4@PC-POP for two analytes. According to the experimental value and the parameters calculated in Table S4, the experimental value of equilibrium adsorption amount of 4-hydroxybenzoic acid and P-cresol were 54.7 mg g^{-1} and 67.7 mg g^{-1}, which is similar to the calculated value from the pseudo-second-order kinetic model (60.6 mg g^{-1} and 71.9 mg g^{-1}). Furthermore, the pseudo-second-order kinetic model provided the more suitable correlation (R^2) (0.997 and 0.995), which means that the chemical adsorption is the main rate determining step.

According to the parameters in Table S5, the adsorption of 4-hydroxybenzoic acid and P-cresol on Fe_3O_4@PC-POP is more similar to Freundlich model. It is because the electrostatic and hydrophobic interaction between Fe_3O_4@PC-POP and two analytes coexist in the extraction process, which is not restricted to the monolayer adsorption.

Performance comparison of Fe_3O_4@PC-POP and commercial sorbents for extraction of the target compounds

Based on the hydrophobicity of P-cresol and charge property of 4-hydroxybenzoic acid in aqueous solution, commercial sorbents C18 and SAX were selected to investigate the extraction efficiency of adsorbent for two analytes at pH = 5.5 buffer. As shown in Fig. 4, the extraction efficiency of Fe_3O_4@PC-POP is superior to those of C18 and SAX adsorbent. In addition, the prime cost of the synthesized materials is about 3.1 RMB/g in the lab scale system, which is far below the price of the commercial adsorbent (the cost of the commercial C18 and SAX are about 18 and 27 RMB/g, respectively). Therefore, the proposed Fe_3O_4@PC-POP material has great superiority than the conventional commercial sorbents.

Adsorption mechanism of Fe_3O_4@PC-POP for metabolites

In order to validate the interaction mechanism between Fe_3O_4@PC-POP and the targeted analytes, the optimal extraction conditions of adsorbent for 4-hydroxybenzoic acid and P-cresol were also predicted, respectively. It can be seen from Tables S6 and S7 and Figs. S11 and S12 that the predicted optimal pH value for extraction of 4-hydroxybenzoic acid and P-cresol is 3.31 and 7.53, respectively. According to the zeta potential of the material (Fig. S5) and the pKa values of the two analytes in Table S8, under the extraction pH of 3.31, Fe_3O_4@PC-POP is positively charged, and the carboxylic acid group of 4-hydroxybenzoic acid can be partly dissociated as negatively charged carboxylate ion. In such a case, the electrostatic interaction can be occurred between the adsorbent and 4-

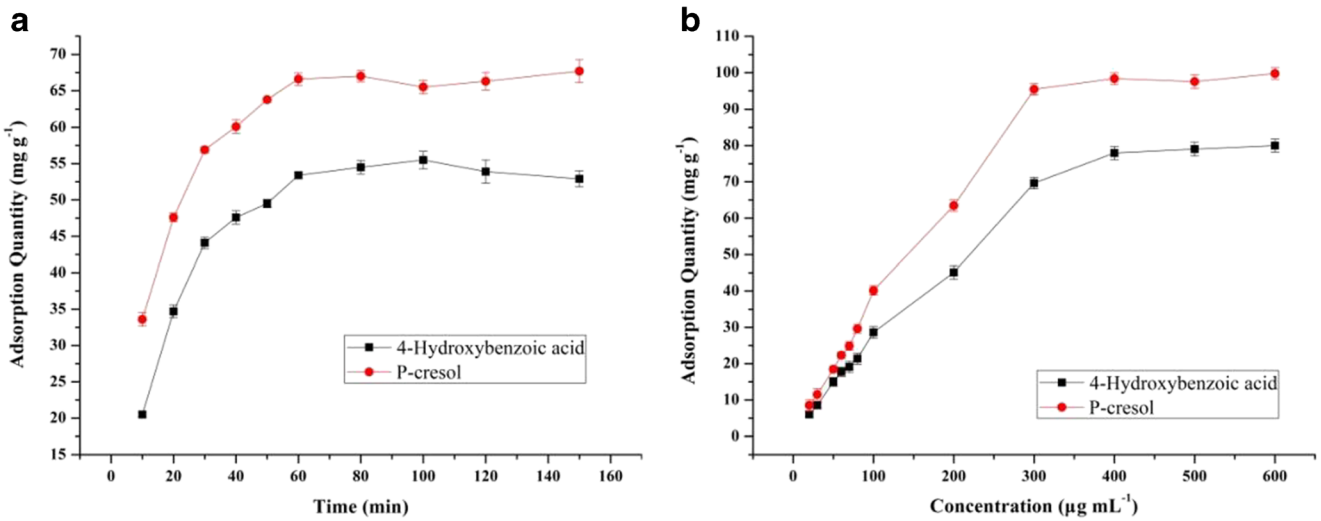

Fig. 3 Adsorption kinetic curves (**a**) and adsorption isotherm (**b**) of two analytes for Fe_3O_4@PC-POP

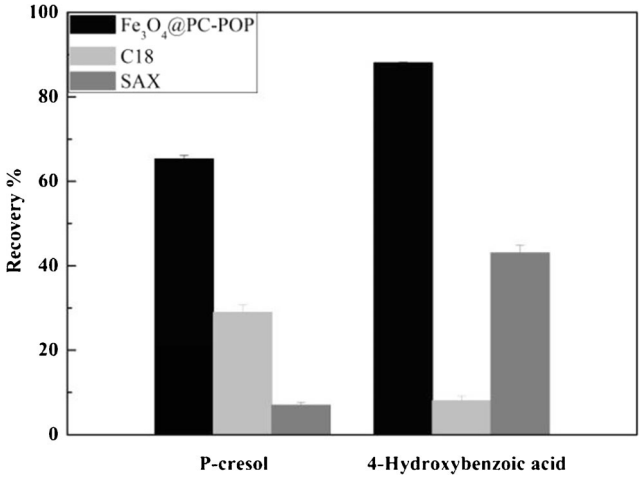

Fig. 4 Comparison of extraction efficiencies of Fe_3O_4@PC-POP and commercial C18, SAX

hydroxybenzoic acid. In theory, the dissociation of 4-hydroxybenzoic acid increases with the increase of solution pH value. However, the increased solution pH will also elicit that Fe_3O_4@PC-POP has the tendency to be negatively charged (Fig. S5), which leads to electrostatic repulsion interaction with 4-hydroxybenzoic acid. It provides a rational theoretical support for above predicted optimal pH of 4-hydroxybenzoic acid. With regard to the compound P-cresol, it is present in molecular form rather than as ion under the investigated conditions. According to the log *P* value of the two analytes and the surface contact angle test of Fe_3O_4@PC-POP, the adsorption of adsorbent for P-cresol should be more inclined to the hydrophobic or other interaction. Based on multiple mechanisms, 7.53 is predicted as the optimal pH for extraction of P-cresol. It is well-known that ionic strength has a great influence on electrostatic interaction [37]. To further verify above deduction, we determined the extraction efficiencies of Fe_3O_4@PC-POP for P-cresol and 4-hydroxybenzoic acid in aqueous solution with different salt concentration. As shown in Fig. S13, with an increase of ionic strength, the extraction efficiency for P-cresol has an inappreciable change, thereby ruling out the possibility of electrostatic interaction between Fe_3O_4@PC-POP and P-cresol. However, it can be observed that increase of ionic strength can lead to a significant decrease in the extraction of 4-hydroxybenzoic acid. The results further illuminate that the adsorption mechanism of Fe_3O_4@PC-POP for 4-hydroxybenzoic acid should mainly be electrostatic interaction. In addition, according to the intuitive data of the higher adsorption behavior of C18 for P-cresol and SAX adsorbent for 4-hydroxybenzoic acid (Fig. 4), the main adsorption mechanism of Fe_3O_4@PC-POP for P-cresol and 4-hydroxybenzoic acid should be attributed to hydrophobic and electrostatic interaction, respectively.

Reusability of Fe_3O_4@PC-POP

Whether the adsorbent material can be reused is very important for practical applications. In this work, the organic porous polymer material is stable in the sample pretreatment process and can be regenerated by simple treatment. As shown in Fig. S14, compared with the result of first extraction, the recovery rate has still remained unchanged after 5 times cycle, indicating that the material has good recyclability.

Analytical performance and application

Quantitative parameters such as linear range, correlation coefficient, limits of detection (LODs), and limits of quantification (LOQs) of the established method under the optimized conditions are displayed in Table 2. The result exhibits the satisfactory linearity for two analytes in the concentration range of 3.0–1000 μg L^{-1} ($R^2 \geq 0.997$). Based on the signal-to-noise ratio (S/N) of 3:1, the LODs of 4-hydroxybenzoic acid and P-cresol are determined to be 0.9 μg L^{-1} and 5.0 μg L^{-1}, respectively, which is below the median of metabolite levels of P-cresol in urine sample (40 μg L^{-1}) [9]. In addition, the established method shows enrichment factor of 34.8 times for P-cresol and 38.7 times for 4-hydroxybenzoic acid compared with the direct injection (20 μL).

Since the analytes as gastric cancer metabolites have only recently been investigated [9], the relevant analytical methods are still rarely developed. To date, only one report is found, and the results are compared with our established method [17]. Table 3 shows that the similar LODs and LOQs are obtained from two methods. However, our developed method is truly applied to determine these metabolites in the real urine samples from healthy people and gastric cancer patients. Fig. S15 shows the chromatograms of urine samples from healthy people and gastric cancer patients before and after enrichment.

Table 2 Analytical parameters of the developed method

Analytes	Linear range (μg L^{-1})	Calibration curves	R^2	LODs (μg L^{-1})	LOQs (μg L^{-1})
P-cresol	20–1000	y = 0.028x + 0.073	0.999	5.0	20
4-Hydroxybenzoic acid	3.0–1000	y = 0.133x + 0.726	0.997	0.9	3.0

Table 3 Comparison of current strategy with previously reported methods

Method	Adsorbent	Samples	Sample volume (mL)	Detection	Mode	LODs (μg L^{-1})	EF	Ref.
MSPE	MA-CD	Water, urine	10	HPLC-DAD	Offline	1.0–5.7	17.48 19.13	[17]
MSPE	Fe_3O_4@PC-POP	Urine	5	UPLC-UV	Offline	0.9–5.0	38.7 34.8	This work

MA-CD magnetic porous cyclodextrin polymer

Table 4 Apparent recoveries of the 4-hydroxybenzoic acid and P-cresol in urine samples from healthy people and gastric cancer patients

	Analytes	Sample	Spiked (μg L^{-1})	Found (μg L^{-1}) (± SD, $n = 3$)	Average apparent recovery (%)	RSD (%) ($n = 3$)
Healthy people		Urine1	0	-	-	-
	P-cresol		50	42.6 ± 1.40	85.3	3.3
			200	224 ± 14.6	112	6.5
			800	814 ± 50.5	102	6.2
		Urine2	0	-	-	-
			50	43.9 ± 1.10	87.8	2.5
			200	183 ± 13.9	91.6	7.6
			800	707 ± 33.2	88.4	4.7
		Urine3	0	-	-	-
			50	53.6 ± 2.40	107	4.5
			200	218 ± 8.50	109	3.9
			800	764 ± 46.6	95.5	6.1
		Urine1	0	-	-	-
	4-Hydroxybenzoic acid		15	13.7 ± 1.00	91.2	7.2
			200	186 ± 10.4	93.1	5.6
			800	743 ± 31.2	92.9	4.2
		Urine2	0	-	-	-
			15	15.4 ± 1.00	100	6.3
			200	178 ± 6.40	88.8	3.6
			800	784 ± 43.1	97.9	5.5
		Urine3	0	-	-	-
			15	16.5 ± 1.20	110	7.1
			200	200 ± 16.8	99.8	8.4
			800	735 ± 30.1	91.9	4.1
Gastric Cancer patients		Urine1	0	45.3 ± 2.90	-	6.4
	P-cresol		50	88.3 ± 4.90	86.0	5.5
			200	270 ± 10.3	113	3.8
			800	868 ± 68.6	103	7.9
		Urine2	0	43.4 ± 2.30	-	5.3
			50	87.9 ± 4.10	89.0	4.7
			200	227 ± 17.3	91.9	7.6
			800	757 ± 40.1	89.2	5.3
		Urine3	0	47.5 ± 2.70		5.6
			50	101 ± 8.30	107	8.2
			200	270 ± 14.0	111	5.2
			800	809 ± 55.0	95.2	6.8
		Urine1	0	81.2 ± 5.80	-	7.2
	4-Hydroxybenzoic acid		15	95.6 ± 8.40	96.0	8.8
			200	267 ± 15.0	92.9	5.6
			800	825 ± 38.8	93.0	4.7
		Urine2	0	75.3 ± 3.20	-	4.2
			15	91.5 ± 5.90	108	6.5
			200	254 ± 12.4	89.2	4.9
			800	860 ± 73.1	98.1	8.5
		Urine3	0	87.3 ± 4.80	-	5.5
			15	104 ± 7.00	110	6.7
			200	288 ± 21.3	101	7.4
			800	826 ± 60.3	92.3	7.3

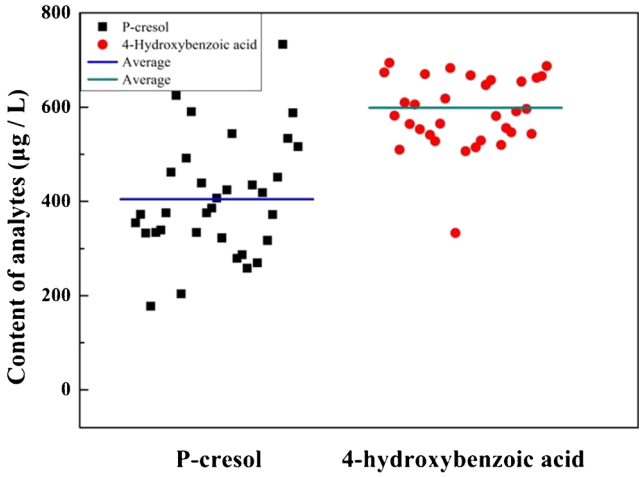

Fig. 5 Content of analytes in urine samples from gastric cancer patients

It can be seen from Fig. S15a and b that both P-cresol and 4-hydroxybenzoic acid cannot be determined from the healthy people's urine samples before and after enrichment. Similarly, the chromatographic peak of two analytes cannot be observed in the urine samples from gastric cancer patients before enrichment (Fig. S15c). However, Fig. S15d shows that two gastric cancer markers can be determined from gastric cancer patients' urine samples after enrichment, indicating that the proposed method can achieve the determination of the targeted analytes at lower levels.

In order to verify the applicability of the developed method, the spiked apparent recovery experiments were performed for each analyte in the urine samples from healthy people's urine and gastric cancer patients. Figure S16 shows the chromatograms of the urine samples from three healthy people and three gastric cancer patients. Table 4 exhibits that the apparent recoveries of P-cresol and 4-hydroxybenzoic acid from the healthy people's urine samples are between 85.3 and 112% and 88.8 and 110% with a relative standard deviation (RSD) of less than 7.6% and 8.4%, respectively. The apparent recoveries of P-cresol and 4-hydroxybenzoic acid from three gastric cancer patients are 86.0–113% and 89.2–110% with RSD values less than 8.2% and 8.8%, respectively. These results illustrate that the developed method is applicable to determine the two gastric cancer markers in real urine samples. It provides a noninvasive technique for diagnosis of gastric cancer or assessment of the patients' status in the cure process.

Finally, the fifteen healthy volunteers and the thirty-three gastric cancer patients were sampled from the outpatient service and the inpatient department in Lanzhou University Second Hospital, and the proposed approach was employed for assay of the two gastric cancer biomarkers in these urine samples. The results illustrate that both P-cresol and 4-hydroxybenzoic acid cannot be determined from the healthy volunteers' urine samples. However, as shown in Table S9, they can be determined, and the average concentrations of P-cresol and 4-hydroxybenzoic acid are 404 μg L^{-1} and 599 μg L^{-1} in the gastric cancer patients' urine samples, respectively. According to the reported literature [9], most of the patients were in Stages III–IV gastric cancer based on the P-cresol content (the pathological stages of gastric cancer were categorized as I–IV based on P-cresol levels ranging from 180 to 500 μg L^{-1}, and the level of 4-hydroxybenzoic acid was not mentioned in the literature). Figure 5 shows the two analytes levels in the obtained urine samples from thirty-three gastric cancer patients.

Conclusion

In this work, a new type of magnetic organic polymer porous composite Fe_3O_4@PC-POP was successfully synthesized and characterized. As the framework is doped with protonizable nitrogen atom and possesses relatively hydrophobic surface properties, it exhibits great promises for the adsorption of two small molecule gastric cancer markers P-cresol and 4-hydroxybenzoic acid mainly based on electrostatic and hydrophobic interaction. Furthermore, the material was successfully used as MSPE adsorbent for enrichment and determination of the targeted analytes in urine samples from the fifteen healthy people and thirty-three gastric cancer patients. The design concept of the proposed adsorbent has flexible and scalable features. It can enlighten us to develop more polymer materials for capturing small molecular disease biomarkers. However, according to the electrostatic and hydrophobic adsorption mechanism, other negatively charged and hydrophobic molecules can also be adsorbed in theory. So there will be some interference with similar properties in the actual sample to affect the analysis results. The specific and selective adsorption properties of the materials should be considered in future work.

Funding information This work was supported by the National Natural Science Foundation of China (NSFC) Fund (No. 21575055) and the Henan Key Laboratory of Biomolecular Recognition and Sensing (HKLBRSK1901).

Compliance with ethical standards

Conflict of interest The authors declare that they have no conflict of interest.

References

1. Wittekmd C, Compton CC, Greene FL et al (2002) TNM residual tumorclassification revisited. Cancer 94:2511–2516
2. Ychou M, Boige V, Pignon JP, Conroy T, Bouché O, Lebreton G, Ducourtieux M, Bedenne L, Fabre JM, Saint-Aubert B, Genève J, Lasser P, Rougier P (2011) Perioperative chemotherapy compared with surgery alone for resectable gastroesophageal

adenocarcinoma: an FNCLCC and FFCD multicenter phase III trial. J Clin Oncol 29:1715–1721
3. Jayanthi VSPKS, Das AB, Saxena U (2017) Recent advances in biosensor development for the detection of cancer biomarkers. Biosens Bioelectron 91:15–23
4. Siegel RL, Miller KD, Jemal A (2015) Cancer statistics, 2015. CA Cancer J Clin 65:5–29
5. Abbas M, Habib M, Naveed M, Karthik K, Dhama K, Shi M, Dingding C (2017) The relevance of gastric cancer biomarkers in prognosis and pre- and post-chemotherapy in clinical practice. Biomed Pharmacother 95:1082–1090
6. Dunn WB, Broadhurst DI, Atherton HJ, Goodacre R, Griffin JL (2011) ChemInform abstract: systems level studies of mammalian metabolomes: the roles of mass spectrometry and nuclear magnetic resonance spectroscopy. Chem Soc Rev 40:387–426
7. Chen JL, Fan J, Lu XJ (2014) CE-MS based on moving reaction boundary method for urinary metabolomic analysis of gastric cancer patients. Electrophoresis 35:1032–1039
8. Liang Q, Wang C, Li B (2015) Metabolomic analysis using liquid chromatography/mass spectrometry for gastric cancer. Appl Biochem Biotechnol 176:2170–2184
9. Chen Y, Zhang J, Guo L, Liu L, Wen J, Xu L, Yan M, Li Z, Zhang X, Nan P, Jiang J, Ji J, Zhang J, Cai W, Zhuang H, Wang Y, Zhu Z, Yu Y (2016) A characteristic biosignature for discrimination of gastric cancer from healthy population by high throughput GC-MS analysis. Oncotarget 7:87496–87510
10. Pijls KE, Smolinska A, Jonkers DM et al (2016) A profile of volatile organic compounds in exhaled air as a potential non-invasive biomarker for liver cirrhosis. Sci Rep 6:19903
11. Luo P, Yin PY, Hua R et al (2018) A large-scale, multicenter serum metabolite biomarker identification study for the early detection of hepatocellular carcinoma. Hepatology 67:662–675
12. Wang J, Zhang T, Shen X, Liu J, Zhao D, Sun Y, Wang L, Liu Y, Gong X, Liu Y, Zhu ZJ, Xue F (2016) Serum metabolomics for early diagnosis of esophageal squamous cell carcinoma by UHPLC-QTOF/MS. Metabolomics 12:116
13. Lu YH, Li N, Gao L et al (2016) Acetylcarnitine is a candidate diagnostic and prognostic biomarker of hepatocellular carcinoma. Cancer Res 76:2912–2920
14. Tian Y, Liu X, Duan J et al (2018) Prediction of chemotherapeutic efficacy in non-small cell lung cancer by serum metabolomic profiling. Clin Cancer Re 24:2100–2109
15. Kashani FZ, Ghoreishi SM, Khoobi A, Enhessari M (2019) A carbon paste electrode modified with a nickel titanate nanoceramic for simultaneous voltammetric determination of ortho- and para-hydroxybenzoic acids. Microchim Acta 186:12
16. Belenguer-Sapia C, Pellicer-Castell E, Vila C et al (2019) A poly (glycidyl-co-ethylene dimethacrylate) nanohybrid modified with β-cyclodextrin as a sorbent for solid-phase extraction of phenolic compounds. Microchim Acta 186:1–11
17. Shi Y, Zhang JY, He J et al (2019) A method of detecting two tumor markers (p-hydroxybenzoic acid and p-cresol) in human urine using a porous magnetic <beta >−cyclodextrine polymer as solid phase extractant, an alternative for early gastric cancer diagnosis. Talanta 191:133–140
18. Wu D, Xu F, Sun B, Fu R, He H, Matyjaszewski K (2012) Design and preparation of porous polymers. Chem Rev 112:3959–4015
19. Jiang JX, Cooper A (2010) Microporous organic polymers: design, synthesis, and function. Topics Curr Chem 293:1–33
20. Budd PM, Butler A, Selbie J, Mahmood K, McKeown NB, Ghanem B, Msayib K, Book D, Walton A (2007) The potential of organic polymer-based hydrogen storage materials. Phys Chem Chem Phys 9:1802–1808
21. Li Z, Yang YW (2017) Creation and bioapplications of porous organic polymer materials. J Mater Chem B 5:9278–9290
22. Zhang W, Aguila B, Ma S (2017) Potential applications of functional porous organic polymer materials. J Mater Chem A 5:8795–8824
23. He J, Xu FJ, Chen Z et al (2017) AuNPs/POPs as a new type of SERS substrate for sensitive recognition of polyaromatic hydrocarbons. Chem Commun 53:11044–11047
24. Qian L, Jian BS, Jian TS et al (2011) Graphene and graphene oxide sheets supported on silica as versatile and high-performance adsorbents for solid-phase extraction. Angew Chem 50:5913–5917
25. Jiang B, Wu Q, Deng N, Chen Y, Zhang L, Liang Z, Zhang Y (2016) Hydrophilic GO/Fe3O4/Au/PEG nanocomposites for highly selective enrichment of glycopeptides. Nanoscale 8:4894–4897
26. Zhang C, Li G, Zhang Z (2015) A hydrazone covalent organic polymer based micro-solid phase extraction for online analysis of trace Sudan dyes in food samples. J Chromatogr A 1419:1–9
27. Wei W, Lu R, Xie H, Zhang Y, Bai X, Gu L, da R, Liu X (2015) Selective adsorption and separation of dyes from an aqueous solution on organic–inorganic hybrid cyclomatrix polyphosphazene submicro-spheres. J Mater Chem A 3:4314–4322
28. He G, Peng H, Liu T, Yang M, Zhang Y, Fang Y (2009) A novel picric acid film sensor via combination of the surface enrichment effect of chitosan films and the aggregation-induced emission effect of siloles. J Mater Chem 19:7347–7353
29. Hu X, Long Y, Fan M et al (2018) Two-dimensional covalent organic frameworks as self -template derived nitrogen-doped carbon nanosheets for eco-friendly metal-free catalysis. Appl Catal B Environ 244:25–35
30. Ma HC, Kan JL, Chen GJ, Chen CX, Dong YB (2017) Pd NPs-loaded homochiral covalent organic framework for heterogeneous asymmetric catalysis. Chem Mater 29:6518–6524
31. Wang H, Wang C, Yang Y, Zhao M, Wang Y (2017) $H_3PW_{12}O_{40}$ /mpg-C_3N_4 as an efficient and reusable bifunctional catalyst in one-pot oxidation-Knoevenagel condensation tandem reaction. Catal Sci Technol 7:405–417
32. Shcherban ND, Mäki-Arvela P, Aho A, Sergiienko SA, Yaremov PS, Eränen K, Murzin DY (2018) Melamine-derived graphitic carbon nitride as a new effective metal-free catalyst for Knoevenagel condensation of benzaldehyde with ethylcyanoacetate. Catal Sci Technol 8:2928–2937
33. Fine AK, Schmidt MP, Martínez et al (2018) Nitrogen-rich compounds constitute an increasing proportion of organic matter with depth in O-i-O-e-O-a -A horizons of temperate forests. Geoderma 323:1–12
34. Dong H, Guo X, Yang C, Ouyang Z (2018) Synthesis of g-C_3N_4, by different precursors under burning explosion effect and its photocatalytic degradation for tylosin. Appl Catal B Environ 230:65–76
35. Faisal M, Ismail AA, Harraz FA, al-Sayari SA, el-Toni AM, al-Assiri MS (2016) Synthesis of highly dispersed silver doped g-C_3N_4 nanocomposites with enhanced visible-light photocatalytic activity. Mater Des 98:223–230
36. Leng Y, Li J, Zhang C, Jiang P, Li Y, Jiang Y, du S (2017) N-doped carbon encapsulated molybdenum carbide as an efficient catalyst for oxidant-free dehydrogenation of alcohols. J Mater Chem A 5:17580–17588
37. Ravindran S, Williams MAK, Ward RL, Gillies G (2018) Understanding how the properties of whey protein stabilized emulsions depend on pH, ionic strength and calcium concentration, by mapping environmental conditions to zeta potential. Food Hydrocoll 79:572–578